Copyright WILEY-VCH Verlag GmbH & Co. KGaA, 69469 Weinheim, Germany, 2016.

NANO MICRO
small

Supporting Information

for *Small*, DOI: 10.1002/smll.201603080

Nanomembrane-Based, Thermal-Transport Biosensor for Living Cells

*Rami T. ElAfandy, Ayman F. AbuElela, Pawan Mishra, Bilal Janjua, Hassan M. Oubei, Ulrich Büttner, Mohammed A. Majid, Tien Khee Ng, Jasmeen S. Merzaban, and Boon S. Ooi**

Nanomembrane-Based, Thermal-Transport Biosensor for Cancer Cells

Rami T. ElAfandy[1], Ayman F. AbuElela[2], Pawan Mishra[1], Bilal Janjua[1], Hassan Obei[1], Ulrich Büttner[3], Mohammed A. Majid[1], Tien Khee Ng[1], Jasmeen S. Merzaban[2] and Boon S. Ooi[1]

SUPPORTING INFORMATION

Photoluminescence (PL) emission from the gallium nitride (GaN) nanomembrane (NM)

PL emission from GaN NMs having three different thicknesses (40, 20 and 10 nm) were measured (FIG. S1). All the NMs with different thicknesses emit PL at the same energy while being excited by the lowest excitation intensity (0.0033 mW/µm^2) indicating no increase in local temperature. As the laser intensity increases, the NMs PL emissions red-shift and the spectral full width at half maximum (FWHM) increases due to a steady state increase in local temperature. The thinner the NM, the longer the red-shift and the larger the FWHM due to a lower thermal conductivity which causes a higher increase in temperature.

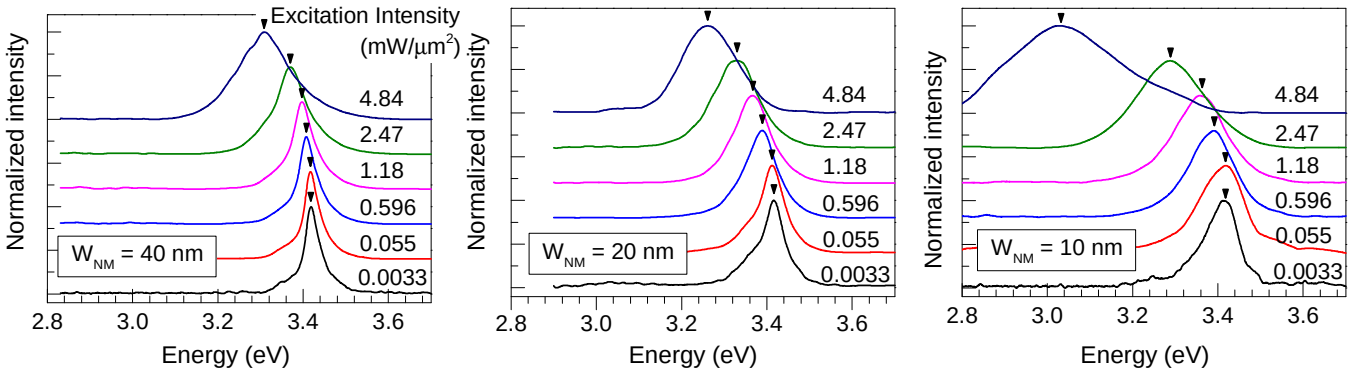

FIG. S1. PL emission from 40, 20 and 10 nm thick GaN NMs. With increasing laser excitation intensity, PL signals measured from 40, 20 and 10 nm thick GaN NMs exhibit a spectral redshift of different magnitudes because of the decrease of the thermal conductivity with decreasing NM thickness.

COMSOL Multiphysics simulation

The cell was modelled as a chamfered cylinder with a 5 µm radius and a 10 µm height. Because water normally accounts for approximately 80 % of the cell's weight, we used water thermal conductivity and diffusivity to model the thermal properties of living cells. Because cells have even lower thermal diffusivities than water, heat energy will be further confined in case of cells. Regarding the thermal properties of gallium nitride

[1]Photonics laboratory, Computer, Electrical and Mathematical Sciences and Engineering, King Abdullah University of Science and Technology (KAUST), Thuwal, 23955-6900, Saudi Arabia, [2]Division of Biological and Environmental Sciences and Engineering (BESE), King Abdullah University of Science and Technology (KAUST), , Thuwal 23955-6900, Saudi Arabia, [3]Microfluidics core lam, Computer, Electrical and Mathematical Sciences and Engineering, King Abdullah University of Science and Technology (KAUST), Thuwal, 23955-6900, Saudi Arabia.

(GaN) and gold (Au), we used the values available in the COMSOL libraries. The following time-dependent heat diffusion equation was solved for the NM/Au microdisc/cell system;

$$\frac{\partial T}{\partial t} = \nabla.(\alpha \nabla T) + \frac{Q}{\rho C_p}$$

where α, ρ, C_p and Q are the thermal diffusivity, density, specific heat capacity at constant pressure and heat source power per unit volume, respectively. The initial temperature was set at 37 °C. Convection cooling from the NM is taken into account by having a column of air on the NM. FIG. S2 contains the simulation results for the temperature depth profile of the NM/ cell system after being heated by a 100 µs long excitation pulse.

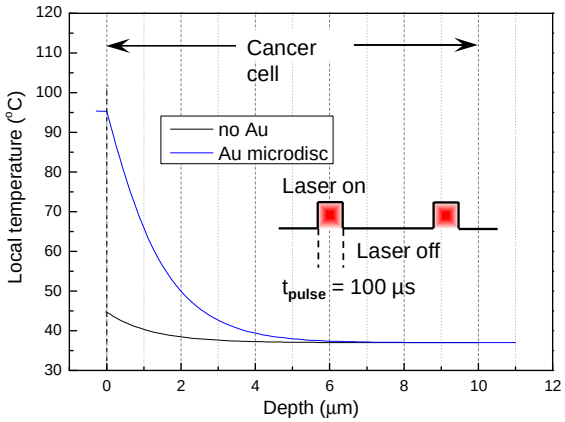

FIG. S2. COMSOL Multiphysics simulation model of a GaN NM attached to a cell while being heated by a laser beam. Temperature depth profile for the case when the NM is in direct contact with the cell and when an Au microdisc is inserted. The laser beam was pulsed at a 100 µs long excitation pulse. Ambient temperature was taken as 37°C in these simulations.

Experimental optical setup

As shown in FIG. S3, 325 nm laser radiation, originating from a helium-cadmium (He-Cd) laser, was first chopped into 7 µs or 100 µs pulses using a Scitec 310CD high-speed optical chopper with an in-house drilled 400 µm wide hole. The generated pulses had a very low duty cycle (1.27×10^{-3}) to ensure that all of the laser-generated heat energy during one pulse is dissipated before the incoming second heating pulse. A set of optical density filters were used to vary the laser radiation intensity from 0.033 to 1.18 mW/µm^2. After locating the Au microdisc, which is attached to the NM, the laser beam was focused to a spot of 3 µm in diameter using a 40x UV objective lens. The sample was left on a thermo-electric controller, set at 37 °C, long enough to reach thermal equilibrium prior to performing the measurement. The photoluminescence emission from the NM, was then collected by the same objective and dispersed by a 2400 line grating onto a charge-coupled device (CCD) camera. Each measurement consisted of collecting the PL emission at different laser radiation intensities and different chopping speeds.

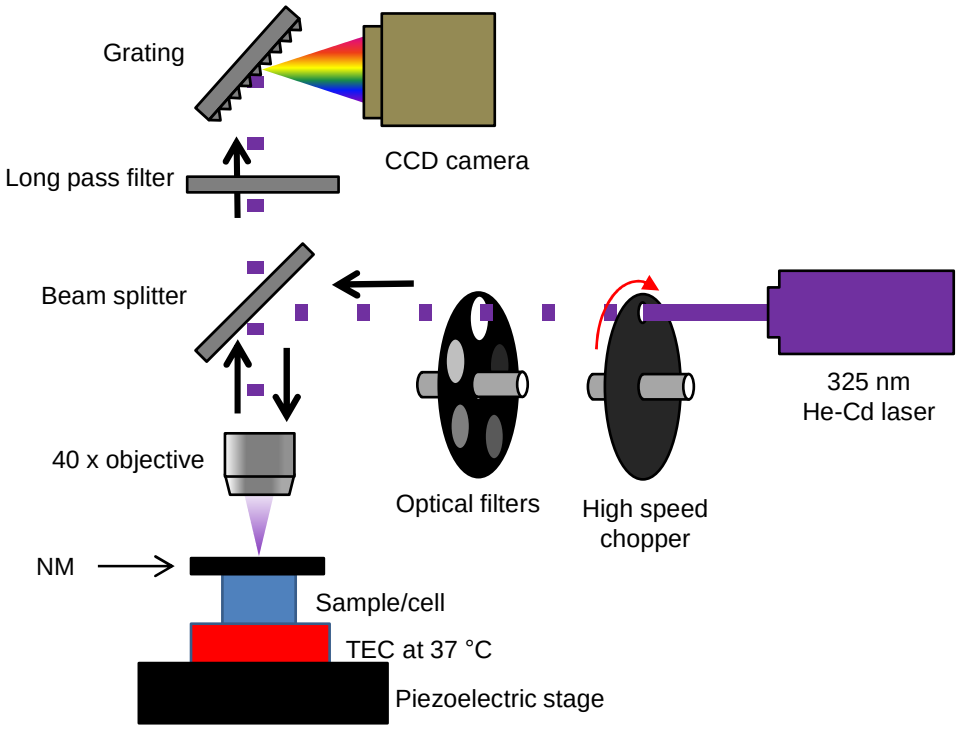

FIG. S3. Experimental setup used to measure thermal diffusivities. Schematic diagram depicting the beam optical path for the excitation 325 nm laser as well as the PL emission from the NMs.

In order to be certain that the NM did not induce cell death; we used trypan blue dye to test cell's viability. FIG. S4a and b show the back light optical image of an MCF7 after the GaN NM was transferred onto it

and the same MCF7 after we incubated the cells in the Trypan blue dye for two minutes, respectively. Dead and live cells were identified by dye inclusion and exclusion, respectively. As imaged in FIG. S4b and c the cell is still considered alive.

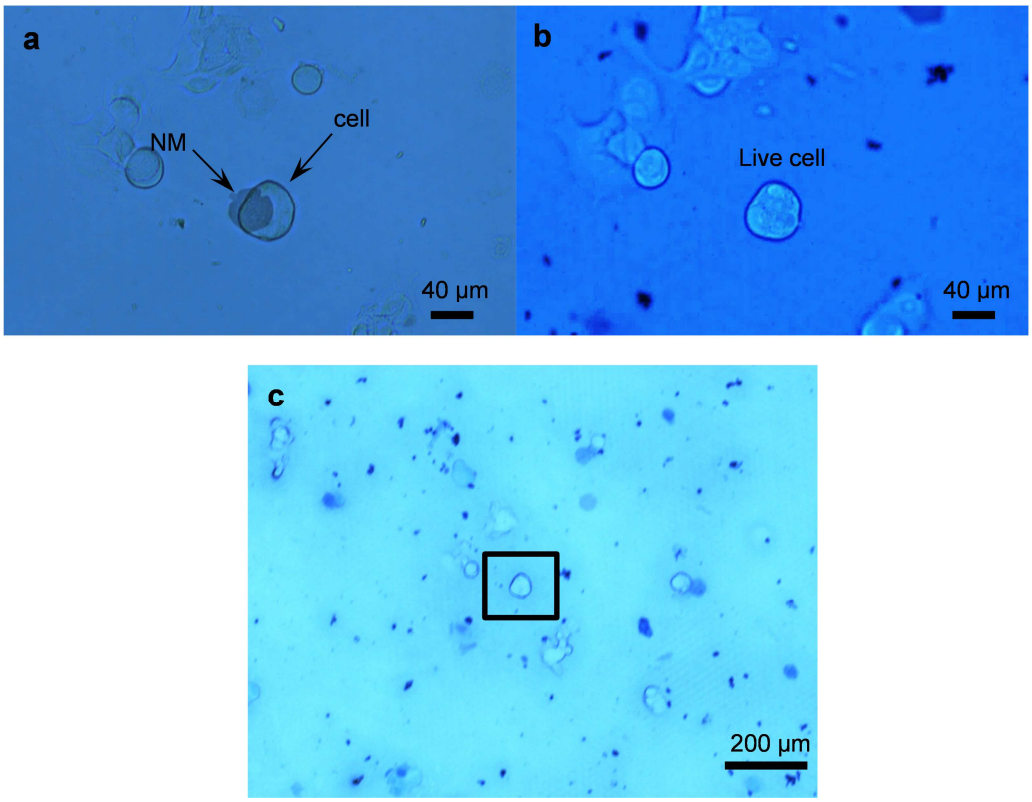

FIG. S4. Assessing cell viability using Trypan blue dye. a) An MCF7 cell, adherent to a glass slide, after the NM has been attached to it. b) After incubating the cell with Trypan blue dye diluted with equal volume of complete culture medium for two minutes, the cell did not absorb the dye through its cell membrane indicating that the cell was still alive. C) the same cell (inside the box) imaged at low magnification.

Since 325 radiation is absorbed within the cell cytoplasm and leads to cell death, we protect the underlying cells by fabricating a 250 nm thick Au microdisc placed underneath the focused laser radiation. FIG. S5 contains the reflection, transmission and absorption curves through a 250 nm thick thin film. As demonstrated, the film transmission of 325 nm radiation is measured to be 0.01 %. Thus, the cell is not affected from the 325 nm excitation laser. In order to be more certain that the cell is protected by the Gold microdisc, we collected the PL spectrum from the GaN NM by focusing the laser on and away from the gold microdisc (red and blue curves in **FIG. S5**b, respectively). As observed, focusing the laser away from the microdisc causes the laser to be absorbed in the cell where it excites a photoluminescence emitting at 2.98 eV while focusing the laser on the microdisc only excites the GaN emission peak (at 3.42 eV) without being absorbed and damaging the underlying cell.

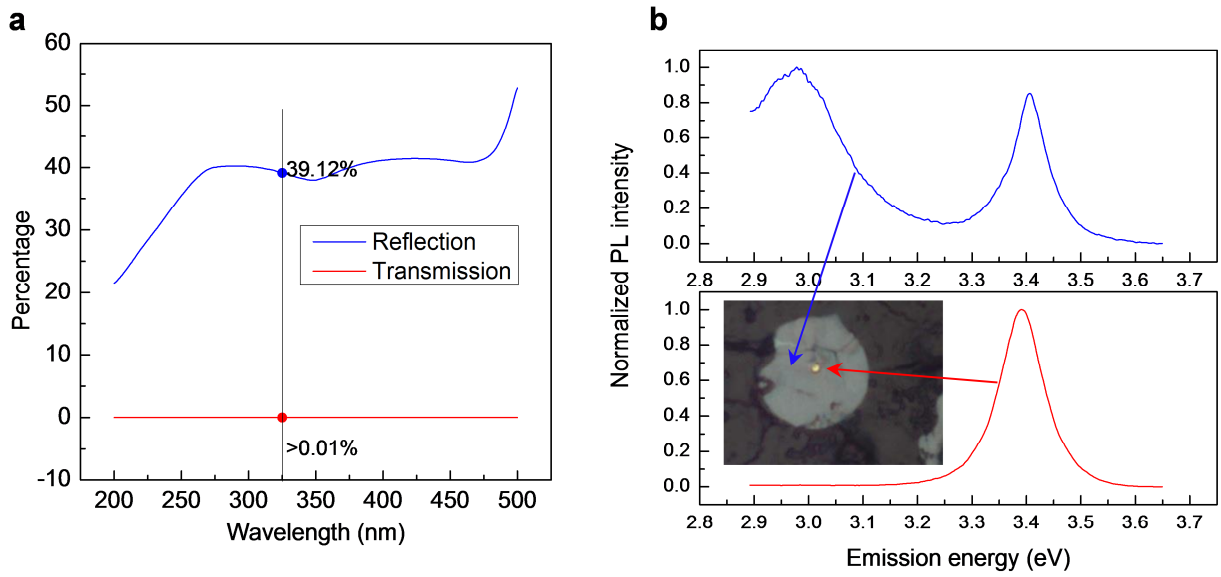

FIG. S5. a)Reflection (blue) and transmission (red) spectrum through 250 nm thick gold. Transmission through 250 nm for 325 nm radiation is negligible. b) PL spectrum measured from the GaN NM though focusing the laser on the gold microdisc (red) and away from the gold microdisc (blue).

Thermal conductivity and diffusivity calculations

Temperature increase in a semi-infinite homogeneous medium by a Gaussian heat source is given by

$$T(t) = RT + A\frac{\sigma^3}{\kappa_{cell}} \times \left(\frac{1}{\sigma} - \frac{1}{\sqrt{\sigma^2 + 2\alpha_{cell}t}}\right)$$

where A and σ are the Gaussian heat source (laser) total power density and standard deviation, respectively; κ_{cell} and α_{cell} are the cell thermal conductivity and diffusivity, respectively; RT represents the surrounding room temperature (kept at 37 °C); and t represents the heating time[1]. In our case, this equation is an approximate solution since it does not include heat lost by convection or radiation. However, in order to account for this discrepancy, the NM is transferred to several material of know conductivity and diffusivities and the PL shift was calibrated. As for the semi-infinite assumption, the heating duration was kept short enough to limit heat diffusion to within the cell and thus preventing the boundary conditions from interfering with the measurements. The instantaneous bandgap emission from GaN, as a function of temperature is given by the Varshni's equation:

$$E_{inst} = E(0) - \frac{\alpha T(t)^2}{T(t) + \beta}$$

Where E(0), α and β are the Varshni's constants. Since our experimental setup utilizes a single laser beam as 'pump' and 'probe', simultaneously, and there is no time gating at the CCD camera, the measured peak emission is the average of the E_{inst} across the heating period.

$$E_{ems}(\tau) = \frac{1}{\tau}\int_0^{\tau} E_{inst}(T)\,dt$$

This equation is correct as long as the PL intensity remains constant during heating which is not the case for GaN. To account for the decreasing intensity of the PL emission, we constructed a weighing function $f(t)$ given by

$$f(t) = \frac{(T_2 - RT)V_2}{\big(T_2 - T(t)\big)V_2 + T(t) - RT}.$$

We derived the values of T_2 and V_2 , which are constants, by placing the NM in a heater, increase the temperature and calculate the corresponding decrease in the PL intensity. Integrating $f(t)$ into $E_{ems}(t)$ we get

$$E_{ems}(\tau) = \frac{\int_0^{\tau} f(T) * E_{inst}(T)\,dt + \tau * E_{inst}(RT)}{\int_0^{\tau} f(T)dt + \tau}$$

The terms outside the integrations ($\tau * E_{inst}(RT)$ and τ) are placed to adjust the constant of integrations.

The adjusted p-values of the thermal conductivity, diffusivity and the latent variable of the different pairs are presented in TABLE S 1. As observed, thermal diffusivity always gives a lower p-value than conductivity demonstrating it's ability to differentiate between different types and subtypes of cancer cells. The MCF-7 and SK-BR03, which are both ductal breast cancers, have thermal properties that are not statistically different.

		p-values		
		κ	α	y'
HeLa	MCF-7	0.592	1.1×10^{-6}	1.62×10^{-7}
HeLa	SK-BR-3	0.364	1.94×10^{-7}	2.84×10^{-10}
HeLa	MDA-MB-231	0.001	2.62×10^{-9}	5.77×10^{-14}
MCF-7	SK-BR-3	0.981	0.495	0.272
MCF-7	MDA-MB-231	0.038	3.7×10^{-4}	1.31×10^{-6}
SK-BR-3	MDA-MB-231	0.094	0.026	1.75×10^{-5}

TABLE S 1 adjuscted p-values of the different pairs based on Tukey's honest significance test.

Materials used for calibration

Prior to measuring the thermal properties of cells, we transferred the NMs onto materials of known thermal diffusivities to calibrate the measured signal. Because the fabrication/growth procedure of any material affects its final thermal diffusivity, we could not rely on standard available thermal diffusivities and had to measure the thermal diffusivities ourselves. The measured thermal diffusivities of the materials, which were measured using laser flash technique, are listed in **TABLE S2**.

Material	Thermal diffusivity (mm^2/s)
Poly(methyl methacrylate) (PMMA)	0.09
Water	0.15
Polyether ether ketone (PEEK)	0.178
Soda-lime glass	0.46

TABLE S2. Measured thermal diffusivities. Using laser flash technique, we measured the thermal diffusivities of different materials used to construct the calibration curve for our novel thermal diffusivity sensing technique.

Heating curves of a single cell

FIG. S6 shows a sample of the measured PL emissions from NMs attached to HeLa and MCF7 cells. At both long (100 µs) and short (7 µs) pulse widths, the PL emission from the NMs attached to the cancer cells emitted at the same peak emission when the excitation intensity was 0.0033 $mW/\mu m^2$ (red curves). As the excitation intensity increased, the PL emission from the NM got spectrally redshifted due to the laser-induced heating (black curves). As observed, for both NMs, the spectral redshift was higher for a 100 µs pulse width than a 7 µs pulse. Furthermore, at both 7 and 100 µs pulses, the NM attached to the MCF7 cell emitted at lower energies than the NM attached to the HeLa cell indicating lower thermal transport properties of the MCF7 cell compared to the HeLa cell.

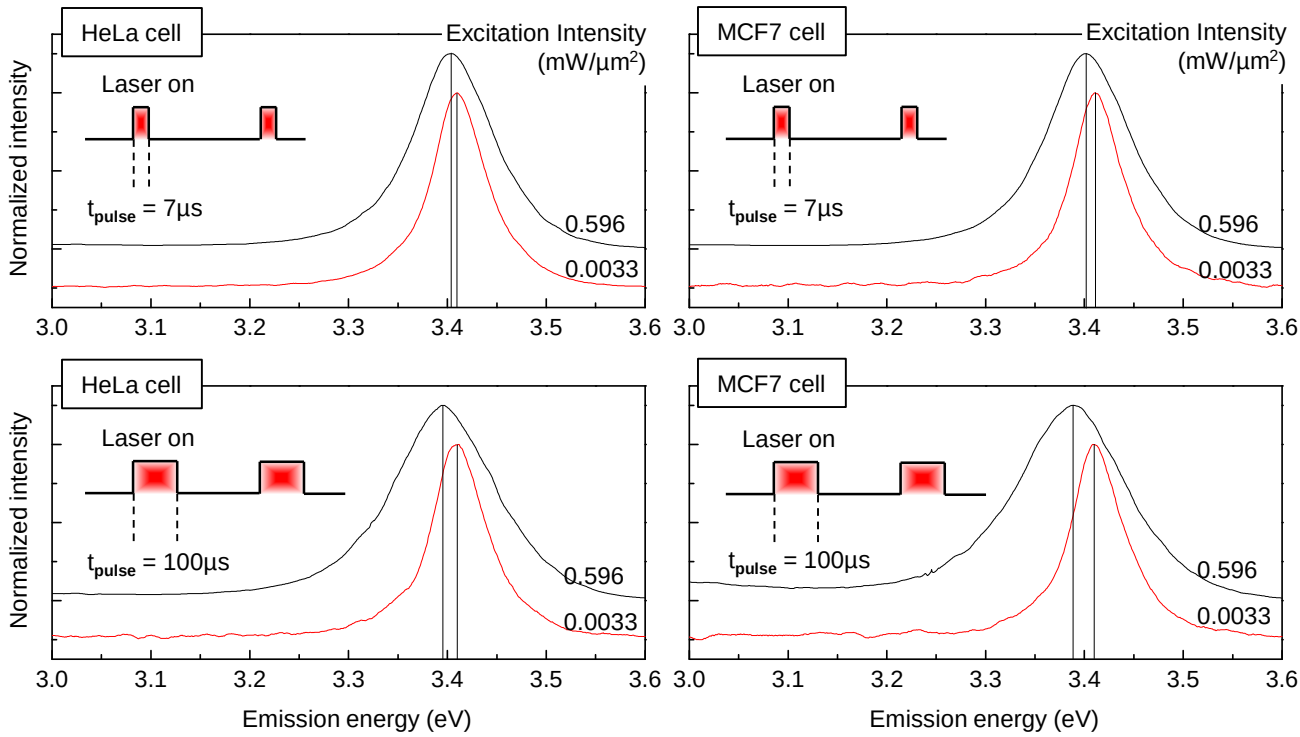

FIG. S6. PL emission from the NM attached to a HeLa (left) and MCF7 (right) cells. Collected PL emissions from a single NM attached to a cell at an increasing laser excitation intensity for long (top) and short (bottom) pulse widths. Black curves were collected at higher excitation energy than red curves.

1 Antonakakis, T., Maglioni, C. & Vlachoudis, V. Closed form solutions of the heat diffusion equation with a Gaussian source. *International Journal of Heat and Mass Transfer* **62**, 314-322, doi:10.1016/j.ijheatmasstransfer.2013.02.061 (2013).